WAVELET ANALYSIS FOR RESOLUTION ENHANCEMENT IN RECURRENCE TRACKING MICROSCOPE

Article · March 2017

CITATIONS
0

READS
34

4 authors, including:

Naeem Akhtar
University of Science and Technology of China
1 PUBLICATION **0** CITATIONS
SEE PROFILE

Aiman Al-Omari
Jerash University
11 PUBLICATIONS **19** CITATIONS
SEE PROFILE

Farhan Saif
Quaid-i-Azam University
110 PUBLICATIONS **775** CITATIONS
SEE PROFILE

WAVELET ANALYSIS FOR RESOLUTION ENHANCEMENT IN RECURRENCE TRACKING MICROSCOPE

Naeem Akhtar[1,4*],Hayat Ullah[2],Aiman al Omari[3] and Farhan Saif[4]

[1]*Hefei National Laboratory for Physical Sciences at the Micro-scale, University of Science and Technology of China, Hefei, Anhui, China, 230026*

[2]*Department of Electronics, Quaid-i-Azam University, Islamabad , Pakistan, 45320*

[3]*Department of Physics, Jerash university, Jerash , Jordan*

[4]*Department of Physics, Quaid-i-Azam University, Islamabad , Pakistan, 45320*

*Corresponding author e-mail: naeemakhtarqau@outlook.com/farhan.saif@fullbrightmail.org

Abstract

We demonstrate that wavelet analysis provides deeper information about the phenomena of quantum recurrences. We apply our analytical results based on continuous wavelet transform (CWT) to modify the resolution of Recurrence tracking microscope (RTM). The information of frequency bands and corresponding fractional revivals make it advantageous to read time of revival and fractional revivals more accurately. Our analytical results show very good agreement with numerical results based on experimental parameters.

Keywords: wavelets,multiscale modeling,recurrence tracking microscope,revival time.

1 Introduction

Position sensors with nano meter resolution is a major area of current research and has achieved a good attention from scientific community [1–4]. Historically, development of electron microscope and scanning probe microscope (SPM), separately based on imaging and sensing of a given sample surface respectively, has been rewarded with Nobel Prize in 1986 [5].

Resolution enhancement of optical microscopes beyond diffraction limit has been acknowledged by Nobel Prize in 2014 [6]. Optical microscopes with enhanced resolution have problem of heating the sample and may damage a sample due to long exposure times. Scanning tunnelling microscope (STM) based on quantum tunnelling phenomena probes a surface with high accuracy [7,8]. It can not work for conducting and non-conducting surfaces in the same way, moreover impurity atoms introduce unwanted structures in scanning. Atomic force microscope (AFM), another important number of SPM, has problem due to diffraction limit.

In 2006, Recurrence Tracking Microscope (RTM), based on the phenomena of quantum recurrences, is suggested [9] which have advantages over STM and AFM. In RTM quantum evolution of a wave packet shows revival behaviour and reappears when it displays maximum constructive interference and therefore partially or completely regains its initial form during temporal evolution. The phenomena of quantum revival have been studied over the past decades in un-driven [10–13] and driven systems [14].

In signal processing the frequency domain of a signal $g(t)$ can be obtained by using Fourier Transform (FT) [15],

$$g(\omega) = \int_{-\infty}^{+\infty} g(t) e^{-2\pi i f t} dt. \tag{1}$$

The FT provides the representative frequency components involve in power spectrum of a signal. However, FT does not give information of time and frequency simultaneously. This is the main drawback of the FT in the analysis of a multiple components signal. In case of multiple component signal it seems more beneficial to reconstruct each component of signal across its frequency. In order to obtain time-frequency representation of a signal simultaneously [16, 17].

The wavelet transform is applied to identify nano topography of crystal surfaces [18, 19] and used for the determination of the birefringence dispersion in optical fibres [20]. Further it has been shown that the use of the wavelet transform can be very effective with atomic force microscope (AFM) data analysis [21]. The wavelet transform is also a very useful technique in filtering of low frequency structures in STM [22], to extract weak signals from a high noise background [23], in analysing quantum wave packet dynamics [24, 25] and in quantum field theory [26–29].

In our work we use the method of continuous wavelet transform (CWT) for the time-frequency analysis of a material wave packet in RTM [11, 12]. We reconstruct each time harmonic of the material wave packet across its frequency, which on one hand increases the conceptual understanding of the quantum recurrences and on other hand increases the resolution of RTM. The CWT, $T_{g(t)}(f,\tau)$, of a signal $g(t)$ can be defined as,

$$T_{g(t)}(f,\tau) = \sqrt{\frac{f}{f_0}} \int_{-\infty}^{+\infty} g(t) h^* \left[\frac{f}{f_0}(t-\tau) \right] dt,$$

$h(t)$ is known as mother wavelet [16] and the ratio $\left(\frac{f_0}{f}\right)$ is the scaling parameter. Let us assume that the wavelet is centred at time zero and oscillates with frequency f_0. The wavelet basis function $h\left[\frac{f}{f_0}(t-\tau)\right]$ has a variable length and width according to frequency f at different stages τ of the signal. The resulting 2D square magnitude display of the transformed function $T_{g(t)}(f,\tau)$ is known as scalogram.

$$h(t) = \pi^{-1/4} e^{2\pi i f_0 t} e^{-t^2/2},$$

where f_0 is the central frequency of the wavelet. To construct the translated and dilated Morlet wavelet we replace t by $\frac{f}{f_0}(t-\tau)$ to get,

$$T_{g(t)}(f,\tau) = \pi^{-1/4} \sqrt{\frac{f_0}{f}} \int_{-\infty}^{+\infty} g\left(\tau + \zeta \frac{f_0}{f}\right) e^{-i f_0 \zeta} e^{\frac{-1}{2}\zeta^2} d\zeta,$$

where $\zeta = \frac{f}{f_0}(t-\tau)$ and $T_{g(t)}(f,\tau)$ is CWT for a signal $g(t)$ by using Morlet wavelet. The layout of paper is as follow: In section-II we briefly explain RTM and calculate the auto-correlation function associated with matter waves. In section-III the time-frequency representation of auto-correlation function is carried out using CWT. We dedicate section-IV to explain the resolution enhancement in RTM by applying the developed time-frequency analysis.

2 Temporal Evolution in RTM

A material wave packet in its time evolution, manifests de-coherence and coherence phenomena as it experiences destructive and constructive interference that leads to quantum recurrences. As the wave packet follows classical evolution it reconstructs itself after a classical period, T_{cl}. Thereafter, the wave packet dynamics displays a gradual increase in destructive interference that leads to periodic collapse. We observe recurrence phenomena in the long time domain which are the manifestation of constructive interference [10].

In Recurrence tracking microscope we propagate a material wave packet which experimentally represents a cold caesium atom moving under the gravitational field [11–13]. The atom bounces over an atomic mirror made up of an evanescent wave above a dielectric surface which is connected with a cantilever. The other end of the cantilever probes the unknown surface. For simplicity we take exponential potential of the evanescent wave as an infinite potential [30, 31]. In order to calculate the temporal evolution of the wave packet we calculate auto-correlation function, defined as

$$A(t) = \sum_n |a_n|^2 e^{-iE_n t/\hbar}. \tag{2}$$

Here, the probability amplitude a_n can be obtained mathematically [33] and E_n defines energy eigenvalue. The energy eigenvalue associated with the triangular well potential can be defined as,

$$E_n = \left(\frac{F^2\hbar^2}{2m}\right)^{1/3} z_n, \tag{3}$$

where z_n are the zero's of Airy function [32] and $F = mg$. In case of large quantum number it can be approximated as $z_n = \left[\frac{3\pi}{2}(n - 1/4)\right]^{2/3}$. Since the distribution $|a_n|^2$ is peaked around average quantum number n_0, therefore we expand the energy eigenvalue around the average quantum number n_0, such that $\Delta n = n - n_0 << n_0$ [10], we have

$$E_n \cong E_{n_0} + \frac{2\pi(n - n_0)}{T_{cl}} + \frac{2\pi(n - n_0)^2}{T_{rev}}, \tag{4}$$

where we have ignored higher powers. The corresponding classical and quantum revival times for RTM are $T_{cl} = 2\sqrt{\frac{2mz_0}{F}}$ and $T_{rev} = \frac{16mz_0^2}{\pi\hbar}$, respectively [12].

In order to study the time evolution we calculate the absolute square of the auto-correlation function defined as,

$$g(t) = \sum_{n,m} |a_n|^2 |a_m|^2 e^{-iE_{nm}t/\hbar}, \tag{5}$$

where $E_{nm} = E_n - E_m$. The auto-correlation function for the material wave packet for a certain fixed position of the cantilever is shown in Fig. 1(a). In next section, we explain revival and fractional revivals in time-frequency domain and plot scalogram, which localizes them in time-frequency plane and determines their order.

3 TIME-FREQUENCY ANALYSIS

The continuous wavelet transform (CWT) for the auto-correlation function $g(t)$ given in equation (5) is obtained as,

$$T_{g(t)}(f,\tau) = \pi^{-1/4}\sqrt{\frac{f_0}{f}}\sum_{n,m}|a_n|^2|a_m|^2 e^{-iE_{nm}\tau/\hbar} I_{nm}, \tag{6}$$

where $I_{nm} = \int_{-\infty}^{+\infty} e^{-\frac{iE_{nm}f_0\zeta}{f}} e^{-2\pi i f_0\zeta} e^{\frac{-1}{2}\zeta^2} d\zeta$. By solving I_{nm} and using Taylor's series expansion of energy eigenvalues for n and m, as given in equation (4) the CWT, $T_{g(t)}(f,\tau)$ gets form as,

$$T_{g(t)}(f,\tau) = v\sum_{n,m} \mid c_{n,m} \mid^2 e^{-ix_{nm}\tau} r_{n,m}. \tag{7}$$

where $v = \pi^{-1/4}\sqrt{\frac{2\pi f_0}{f}}$, $x_{nm} = 2\pi(n-m)\left[\frac{1}{T_{cl}} + \frac{n+m-2n_0}{T_{rev}}\right]$, $\mid c_{n,m} \mid^2 = \mid a_n \mid^2 \mid a_m \mid^2$ and $r_{n,m} = Exp\left[-\frac{1}{2}\left(2\pi f_0 + \frac{f_0}{f}x_{nm}\right)\right]^2$.

We perform a frequency domain analysis of the auto-correlation by taking Fast Fourier Transform (FFT). The Fast Fourier Transform (FFT) is an efficient algorithm of generating Fourier Transform (FT). The main advantage of FFT is its shorter execution time [34], which it gets by decreasing the number of calculations needed to analyses a waveform.

We plot the FFT of auto-correlation function, which provides frequency components that exist in auto-correlation function, shown in Fig. 1(b). Each component of auto-correlation function can be reconstructed across its frequency which helps to understand the role of frequency in quantum recurrence phenomena. Across each frequency band, as shown in Fig. 1(b), there exists a time harmonic which can be reconstructed by using CWT as given in equation (7).

The CWT, $T_{g(t)}(f,\tau)$, of the material wave packet maps partial fractional revivals across their corresponding frequency bands as shown in Fig. 1(c). This manifests the role of favorable frequencies which contribute to fractional revivals of the wave packet. The sharp peaks and neighboring patches in the scalogram across different frequencies and times identify changes in amplitude of auto-correlation function over time. Each sharp peak and corresponding patch appear in time-frequency distribution correspond to a specific partial fractional revival of the wave packet.

The main advantage obtained from the continuous wavelet transform (CWT) is the reconstruction of the auto-correlation function for specific frequency band and localization of fractional revivals in time-frequency plane. It is important to note that the maximum value of the transformed function $T_{g(t)}(f,\tau)$, as given in equation (7) is at $f = -\frac{x_{nm}}{2\pi}$. Therefore we get,

$$f = (m-n)\left[\frac{1}{T_{cl}} + \frac{m+n-2n_0}{T_{rev}}\right]. \tag{8}$$

By setting $n = n_0$ and $m = n_0 + y$, we get

$$f = \frac{y}{T_{cl}}\left[1 + y\frac{T_{cl}}{T_{rev}}\right]. \tag{9}$$

Under approximation $\frac{T_{cl}}{T_{rev}} << 1$, the central frequency of each frequency band as shown in Fig. 1(b) and (c) can be obtained as follow,

$$f = \frac{y}{2}\sqrt{\frac{g}{2z_0}}, \tag{10}$$

where y is a positive integer such that $y = 1, 2, 3, 4 \ldots$.

The coherent addition of terms as given in equation (6) would requires that the terms corresponding to time dependent exponential is independent of n and m i.e, $\tau E_{n,m} = \tau E_{n',m'}$. Hence, the time τ at which these terms add-up coherently to give a peak structure is,

$$\tau = \frac{s}{2y} T_{rev}, \tag{11}$$

where s is an integer such that $s = 1, 2, 3....$ The central frequency of the lowest frequency band can be obtained by setting $y = 1$ in equation (10). The time $\tau = (s/2)T_{rev}$ corresponding to lowest frequency band that defines specific set of partial fractional revivals as shown in Fig. 2(a). Similarly, the set of partial fractional revival occurs across next frequency band($y = 2$) corresponds to $\tau = (s/4)T_{rev}$ are shown in Fig. 2(b). This process can be extended for higher frequency bands as shown in Fig. 2(c)-(d).

Across each frequency band there is a specific set of the partial fractional revivals. Hence, we conclude that equations (10) and (11) respectively, provide required resolution in frequency and measurement of time to reconstruct fractional revivals in the auto-correlation function. A partial fractional revivals seem

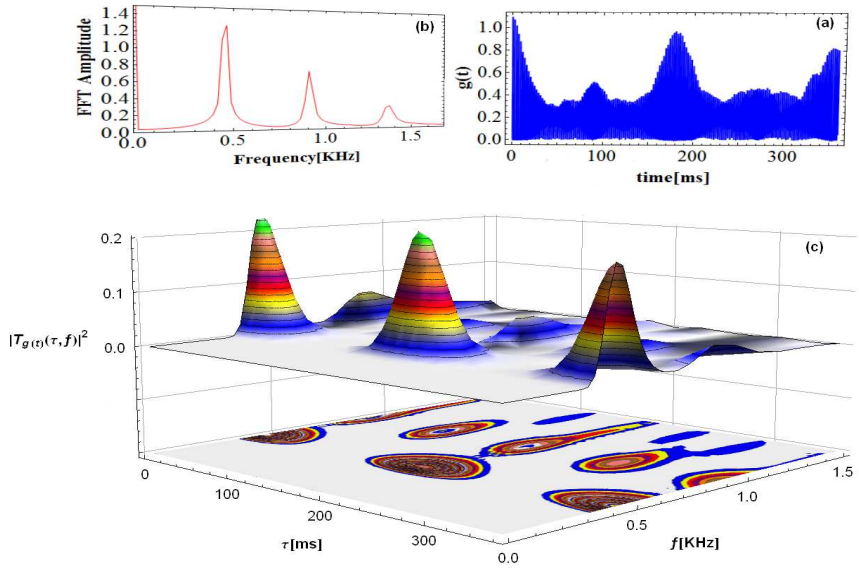

Figure 1: (a) The auto-correlation function of a material wave packet in recurrence tracking microscope. We placed a Gaussian wave packet at $z_0 = 5.65$ μm with $\Delta z = 0.226$ μm above the surface of the optical crystal at $t = 0$ [11, 30]. For the case of caesium (Cs) atom corresponding classical and revival times occurs at 2.14 ms and 348 ms, respectively (b) FFT of the auto-correlation function determines all spectral components (c) Time-frequency representation of the auto-correlation function by using CWT, which explains partial part of a fractional revival across corresponding frequency bands ($|T_{g(t)}(\tau, f)|^2$ is scaled by 10^{-3}).

to be more prominent, which help to identify exact location of a fractional revival. Time-frequency analysis provides a detailed information about the role of constructive and destructive interference in quantum recurrences. The constructive and destructive interference occurs among time series harmonics as shown in Fig. 2(a)-(d), and results in periodic collapses and revival of the wave packet.

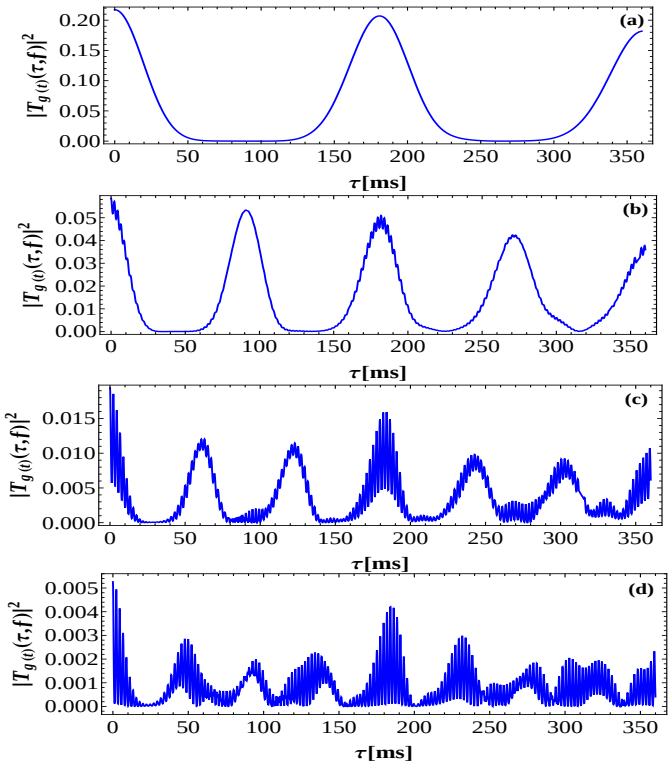

Figure 2: The distribution $|T_{g(t)}(\tau, f)|^2$ is plotted in (a), (b), (c) and (d) for $f = 0.467,\ 0.935,\ 1.401$ and 1.869 (in units of KHz), respectively ($|T_{g(t)}(\tau, f)|^2$ is scaled by 10^{-3}).

4 Resolution Enhancement in RTM

The change in initial height of atom above the atomic mirror modifies revival time. In RTM variation of revival time during an experiment measures nano structures on the surface. The revival of the wave packet, T_{rev}, corresponds to the initial height z_0 that varies as the cantilever moves up or down due to the nano structures on the surface. The uncertainty ΔT in measurement of revival time is proportional to the uncertainty in position of nano structures Δz_0. We express Δz_0 as,

$$\Delta z_0 = \gamma \Delta T, \tag{12}$$

where $\gamma = \frac{z_0}{2T_{rev}}$. The uncertainty in position of the cantilever corresponds to better measurement of size of nano structures on the sample surface. We write it as,

$$a = a^1 + \Delta z_0 \tag{13}$$

where a^1 is the size of nano structures a with a certain uncertainty Δz_0. The uncertainty in partial fractional revivals corresponding to higher frequency bands reduces drastically, which as a results make the time of revival measurements more certain, this leads to a higher resolution in the measurements of the size of nano structure, a. In Table 1, we calculate ΔT and Δz_0 for partial half-fractional revival

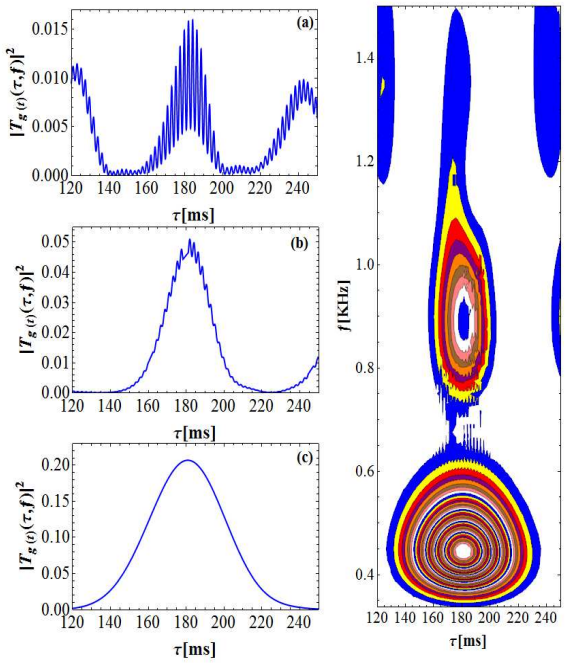

Figure 3: (Left Panel) The peaks corresponding to partial half fractional revival are shown as a function of time τ. The uncertainty around the revival time, ΔT is large for lowest frequency band (c), whereas it reduces gradually for higher frequency bands as obvious in (b) and (a). (Right panel) A section of the scalogram shows partial half-fractional revival in frequency-time plane.

S.No	Frequency(KHz)	ΔT(ms)	Δz_0(nm)
1	0.46	$\cong 5$	$\cong 4$
2	0.93	$\cong 2$	$\cong 1.96$
3	1.8	$\cong 1$	$\cong 0.9$
4	3.6	$\cong 0.7$	$\cong 0.68$

Table 1: We tabulate the uncertainty, ΔT, in partial half-fractional revival calculated at $(3/4)|T_{g(t)}(\tau, f)|^2$ and Δz_0 is the corresponding uncertainty in measurement of size of nano structure across relevant frequency bands.

across various frequency bands. It has been observed that across higher frequency bands ΔT and as a consequence Δz_0 gradually decreases that makes partial half fractional revival more localized around its occurrence time as shown in Fig. 3(a)-(d).

We operate the device around four different values of frequency as shown in Table. 1. As we switch the device to higher frequency the quantity Δz_0 reduces,and hence as a result the resolution of RTM becomes better.

Acknowledgments

Naeem Akhtar acknowledges the CSC fellowship for financial support.

References

[1] P Brault, J Strarck and P B Beauvillian, Phys.Rev.Lett. 76,459 (1996).

[2] Gerd Binnig, Calvin F Quate and Ch Gerber, Phys.Rev.Lett. 56,930 (1986).

[3] David B Williams and C Barry Carter,Springer (1996).

[4] M Auzinsh, Dmitry Budker, DF Kimball, SM Rochester, JE Stalnaker, AO Sushkov and VV Yashchuk, Phys.Rev.Lett. 93,173002 (2004).

[5] Gerd Binnig and Heinrich Rohrer, Rev. Mod. Phys. 59,615 (1987).

[6] Eric Betzig, Stefan W Hell and William E Moerner. The Nobel Prize in Chemistry 2014.

[7] C Julian Chen. Introduction to scanning tunnelling microscopy. Oxford University Press (2008).

[8] Volker Westphal and Stefan W Hell., Phys.Rev.Lett. 94,143903 (2005).

[9] Farhan Saif, Phys.Rev.A, 73,033618 (2006).

[10] Richard W Robinett, Phys. Rep., 392,1119 (2004).

[11] C. G. Aminoff, A. M. Steane, P. Bouyer, P. Desbiolles, J. Dalibard and C. Cohen-Tannoudji, Phys. Rev. Lett. 71,3083 (1993).

[12] Wen-Yu Chen and G. J. Milburn, Phys.Rev.A, 51,2328 (1995).

[13] Soding, R Grimm, and Yu B Ovchinnikov, Opt. Commun., 119,652 (1995).

[14] Farhan Saif, J Opt B Quantum Semiclassical Opt. 7,116 (2005).

[15] Ronald N Bracewell. The Fourier transform and its applications. McGraw-Hill Series in Electrical Engineering, Networks and Systems (1986).

[16] Stephane Mallat. A wavelet tour of signal processing. Academic press (1999).

[17] Francois Auger, Patrick Flandrin, Paulo Goncalves, and Olivier Lemoine. Time-frequency toolbox,‘ CNRS France-Rice University,(1996).

[18] Mingjun Chen, Qilong Pang, Jinghe Wang and Kai Cheng, International Journal of Machine Tools and Manufacture, 48,905 (2008).

[19] HX Wang, WJ Zong, Tao Sun, and Q Liu. Applied Surface Science, 256,5061 (2010).

[20] M Grabka, S Pustelny, P Mergo, and W Gawlik, Opt. Express, 20,13878 (2012).

[21] P Klapetek and I Ohlidal. Applications of the wavelet transform in AFM data analysis, (2005).

[22] P Brault, JL Starck, and P Beauvillain. Characterization of nano-structures STM images with the wavelet and ridge-let transforms, (2003).

[23] Wensheng Cai, Liya Wang, Zhongxiao Pan, Jian Zuo, Cunyi Xu, and Xueguang Shao, J. Raman Spectrosc., 32,207 (2001).

[24] Suranjana Ghosh and J Banerji, J.Phys.B: At.Mol.Opt.Phys, 40,3545 (2007).

[25] Sid-Ahmed Yahiaoui and Mustapha Bentaiba, "arXiv preprint arXiv:1502.08007" (2015).

[26] Gavin K Brennen, Peter Rohde, Barry C Sanders, and Sukhwinder Singh. Multiscale quantum simulation of quantum field theory using wavelets. Phys.Rev. A, 92,032315 (2015).

[27] Fatih Bulut, and Wayne Polyzou, Phys. Rev. D 87, 116011 (2013).

[28] Mikhail V. Altaisky, SIGMA, 3,105 (2007).

[29] M. V. Altaisky, and N. E. Kaputkina, Phys. Rev. D 88, 025015 (2013).

[30] Julio Gea-Banacloche, Am. J. Phys., 67,776 (1999).

[31] MA Doncheski and RW Robinett, Am. J. Phys., 69(quantph/0307046):1084 (2003).

[32] Olivier Vallee and Manuel Soares. Airy functions and applications to physics. Imperial College Press, (2004).

[33] William H Mather and Ronald F Fox, Phys.Rev A 73, 032109 (2006).

[34] The Scientist and Engineer's Guide to Digital Signal Processing By Steven W. Smith, Ph.D.